

# Electronic band structure of cubic CdSe determined by angle-resolved photoemission: Cd 4*d* and valence-level states

K. O. Magnusson

*Department of Physics, University of Karlstad, S-651 88 Karlstad, Sweden*

G. Neuhold\* and K. Horn

*Fritz-Haber-Institut der Max-Planck-Gesellschaft, D-14195 Berlin, Germany*

D. A. Evans

*Athrofa Gogledd Ddwyrain Cymru (NEWI), Clwyd, United Kingdom*

(Received 15 September 1997)

The valence-band structure of epitaxially grown cubic CdSe along the  $\Gamma$ -*K*-*X* direction is determined experimentally using angle-resolved photoelectron spectroscopy on the basis of the free-electron final band model. In the upper valence band the three main branches are determined from normal emission spectra over the range from 15 to 90 eV photon energy, and are found to conform with the general shape expected from this class of materials. The Cd 4*d* level exhibits considerable dispersion, which is reflected in the spectra. The experimental bands are compared with several calculations based on different schemes, and best agreement with respect to dispersion and binding energies is found for a calculation that takes into account electron self-interaction and relaxation. [S0163-1829(98)00415-9]

## I. INTRODUCTION

The characterization of the electronic band structure of II-VI semiconductors is of crucial importance for a better understanding of this important class of materials, which have recently attracted much interest in view of their potential application in novel light-emitting devices.<sup>1</sup> Rapid progress has been made in epitaxial growth of II-VI materials of high quality, and the growth of metastable films of the cubic conformation of several II-VI semiconductors has been reported.<sup>2-4</sup> This has opened the way to performing a comparison of the electronic structure of one particular material in two different crystal conformations, i.e., the cubic (sphalerite) and the wurtzite phase (see, e.g., Refs. 5 and 6). These are similar in that both have a tetragonal coordination with their nearest neighbors, and nearly identical distances with their second nearest neighbors. In spite of these similarities, a recent investigation of electronic transitions using spectroscopic ellipsometry has shown that there are significant differences in the dielectric function of these two crystal structures. It is therefore of interest to compare the valence-band structure in the two crystallographic phases. Here we report on cubic CdSe, grown epitaxially on cleaved GaSb(110) surfaces. Previous results have dealt with the characterization of the epitaxial growth and the determination of the valence band offset in this system.<sup>7</sup> The valence-band structure of the II-VI semiconductors differs in one important aspect from that of the III-V group of semiconductors, in that the cation *d* states are much closer in energy to the upper valence bands, and are thus expected to have a much stronger interaction with these. In fact, recent quasiparticle calculations for CdS using the *GW* approximation have shown that the full cationic shell with main quantum number  $n=4$  must be taken into account in order to provide a description that shows good agreement with experiment.<sup>8</sup>

This is particularly evident in the energy of the cation *d* level, which may show deviations from the experimentally determined binding energy of up to 4 eV if such corrections are not taken into account. Our present study extends this comparison to CdSe; the data are also useful for a test of the calculation scheme by Pollmann and co-workers based on their self-interaction and relaxation-corrected pseudopotentials (SIRC-PP), which has been used to study the electronic structure of many II-VI compound semiconductors.<sup>9</sup>

## II. EXPERIMENT

All experiments were carried out in an ultrahigh vacuum photoelectron spectrometer with a base pressure of about  $8 \times 10^{-11}$  mbar, equipped with a high resolution angle-resolving electron energy analyzer (HA 50 from VSW Ltd., GB) with an angular resolution of about  $2^\circ$  full angle, a cleavage tool, sample load lock, temperature-controlled manipulator which allowed cooling and heating of the sample, molecular beam epitaxy (MBE) cells, and a low-energy electron diffraction (LEED) optics (Omicron GmbH, Germany) for the study of overlayer crystallinity. Crystals of GaSb (MCP Ltd., Great Britain), undoped, with a carrier concentration of  $1.3 \times 10^{17} \text{ cm}^{-3}$  were oriented and cut to be cleaved using the double wedge technique. CdSe with 99.9999% purity (Crystal GmbH, Berlin) was deposited from one water-cooled MBE cell at temperatures of around 500 °C, leading to growth rates of about 0.1–0.5 nm/min. Soft x-ray photons from the BESSY (Berliner Elektronenspeicherring-Gesellschaft für Synchrotronstrahlung mbH) storage ring were dispersed by the TGM 4 toroidal grating monochromator. The system provided an overall resolution of about 70–150 meV for photon energies between 12.5 and 100 eV. All spectra shown were recorded in normal emission. The valence-band maximum was determined through linear extrapolation of the leading edge of the spectra. Over-

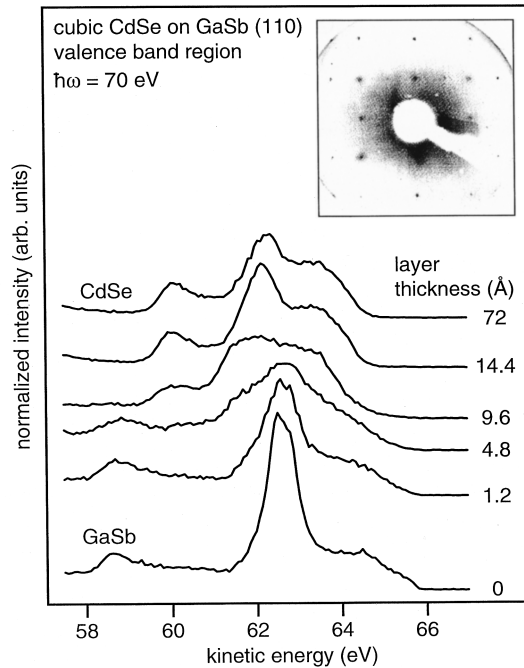


FIG. 1. Angle-resolved photoelectron spectra of the valence bands of clean GaSb(110) and after increasing depositions of CdSe, showing changes in the valence-band structure as the cubic CdSe layer develops. The smaller overall width of the upper valence band of CdSe as compared to GaSb can be directly seen from the data. The inset shows a LEED pattern from a 107-Å-thick CdSe film, recorded at an electron energy of 97.8 eV.

layers were grown, as previously described,<sup>7</sup> on several different substrates in order to establish the optimal growth temperature of 100 °C, characterized by a minimum amount of interface reaction as judged from the Ga 3*d* and Sb 4*d* core levels, and the quality of the LEED diffraction pattern.

### III. RESULTS AND DISCUSSION

The emerging valence-band signature of cubic CdSe, recorded from layers evaporated onto a freshly cleaved sample of GaSb(110), is shown in Fig. 1. Here, spectra were taken from a clean GaSb(110) surface and different thicknesses of epitaxially grown CdSe. Epitaxial growth being demonstrated by the LEED diffraction pattern shown in the inset, recorded from a 107-Å-thick layer at an electron energy of 97.8 eV; the spot pattern displays the correct symmetry for a cubic (110) face, and the spots are sharp with a low diffuse background. The overall shape of the valence band of CdSe has a certain similarity with that of GaSb, in that a broad structure near the VBM is followed by a central peak and a smaller peak at higher binding energies; the main difference compared with GaSb is that the overall bandwidth is much smaller. With substrate band bending upon overlayer formation being rather small,<sup>7</sup> the presence of a large valence-band offset can also be inferred from Fig. 1, since the onset of the valence-band maximum (VBM) occurs at much higher binding energies. The sharp center peak in clean GaSb stems from a direct transition with a large matrix element at this particular photon energy (70 eV), and its gradual extinction by overlayer growth indicates that, even at 14 Å thickness,

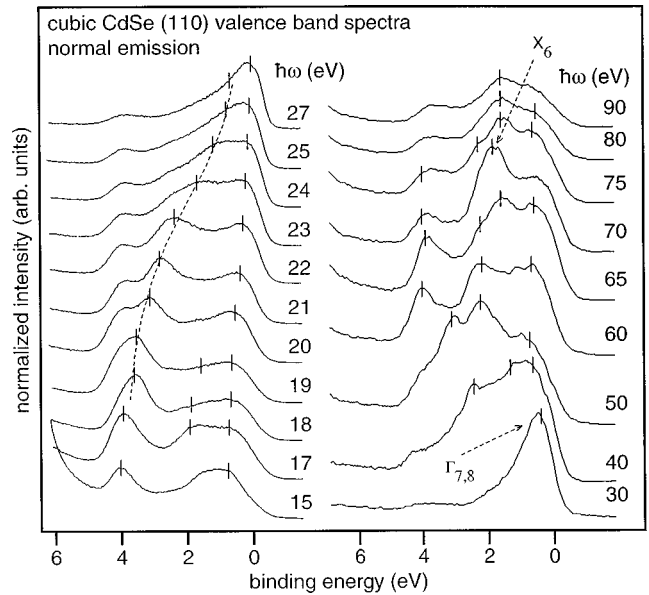


FIG. 2. Series of spectra recorded from cubic CdSe(110) in normal emission, i.e., along the  $\Gamma$ -K-X line, for different photon energies as indicated. Note the large dispersion of the bottom peak (indicated by the dashed line) in the series from 17- to 30-eV photon energy. The  $\Gamma$  point is reached for transitions near the VBM at a photon energy of 30 eV, and the  $X_6$  point for the intense peak in the 70-eV spectra.

the spectrum is already dominated by CdSe features. For a determination of the experimental valence-band structure along the high-symmetry direction normal to the (110) surface, spectra for different photon energies in normal emission along a high-symmetry direction are needed; these are shown in Fig. 2, recorded in the range  $15 < h\nu < 90$  eV. The gradual changes seen in this data set, in particular the clear binding energy variation of the second peak for photon energies between 20 and 30 eV, give convincing evidence for the fact that these spectra are dominated by direct, i.e.,  $\mathbf{k}$ -conserving transitions. In fact, it is evident from the narrowing of the entire spectrum as the photon energy is increased from 20 to 30 eV, that the dispersing band moves towards the VBM and is close to it for a photon energy of 30 eV. The small stationary shoulder at about 4-eV binding energy is due to indirect, i.e., non- $\mathbf{k}$ -conserving transitions from the high density of states of the band of  $\Gamma_{7,8}$ - $X_6$  symmetry between the  $K$  and  $X$  points; similar features are observed in the spectra from other II-VI and III-V semiconductor surfaces.<sup>10-12</sup> This suggests that the photon energy at which the bands are closest to the VBM corresponds to transitions at the  $\Gamma$  point. We assign the dispersing peaks in these spectra to direct,  $\mathbf{k}$ -conserving transitions along the  $\Gamma$ -K-X line from the initial state bands to free-electron final bands,<sup>13</sup> which disperse according to  $E_f = (\hbar^2/2m)(k+G)^2 - V_0$ , where  $E_f$  is the final state energy,  $G$  a reciprocal lattice vector,  $k$  the momentum of the photoelectron, and  $V_0$  the inner potential of the solid. Combined with energy conservation  $E_f - E_i - \hbar\omega = 0$ , the initial band dispersion  $E_i(k)$  can be directly determined from the binding energies of the peaks in the spectra. One problem that has adversely affected more precise band structure evaluations so far is the determination of peak energies. The valence-band spectra cannot

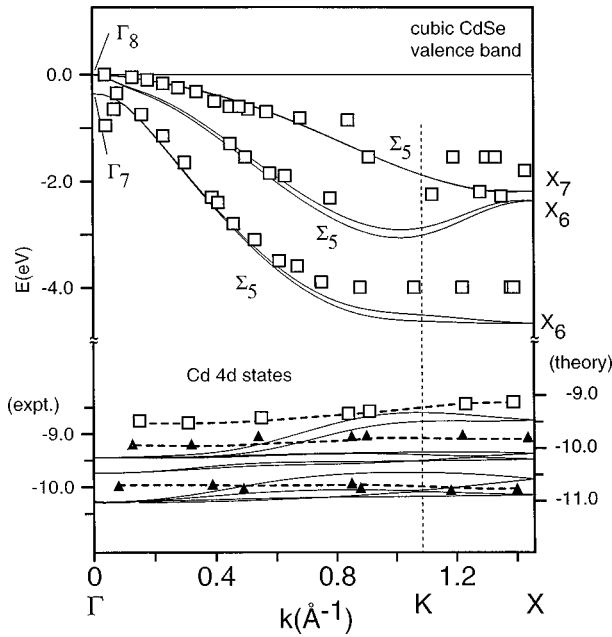


FIG. 3. Experimental band structure of cubic CdSe as determined from spectra such as shown in Fig 2, on the basis of the free-electron final-state model. The thin solid lines are bands calculated within the SIRC-PP scheme by Vogel (Ref. 9). The lower part shows the region of the Cd 4d emission, where the upper and lower experimental points are estimates of the width of the spectral feature. Note that for this region, the experimental and theoretical results were shifted to compare the width of the bands, such that the left-hand energy scale applies to the experimental data, while the right-hand scale applies to the calculation results.

be readily fitted in terms of a parametrized model function through a least-squares algorithm, as is often done in the core-level region, since the model function and the influence of background and indirect transitions are not known. Hence we have to assign peak energies to intensity maxima and shoulders such as indicated by the vertical lines in Fig. 2. The best choice for the only free parameter for band determination, the inner potential  $V_0$ , can be determined from the  $E(k)$  data near critical points, but a good estimate can already be made on the basis of the fact that all bands seem to be close to the VBM at  $\hbar\omega = 30$  eV. Note that in our energy distribution curves, different energies in the curves correspond to different  $\mathbf{k}$  values, but in view of the narrow spread of the valence bands ( $\sim 4$  eV) this is a minor correction,

which is in fact taken into account in the numerical evaluation of the experimental bands shown in Fig. 3. Here, a value of 5.0 eV for the inner potential  $V_0$  was used, which is close to the value of 3.5 eV arrived at in other studies of II-VI semiconductors such as the CdSe(11 $\bar{2}$ 0) surface<sup>14</sup> and 6.0 eV for CdS(110).<sup>6</sup> The peaks identified as direct transitions are indicated as open squares. If we assume the  $G = (2, 2, 0)$  reciprocal lattice vector to be dominant in the direct transitions in the spectra, the calculated critical points are at  $E_f = 29.6$  eV for the  $\Gamma$  point and 68.3 eV for the X point; the next  $\Gamma$  point is not within reach of the photon energies available for this study. The 70-eV spectrum in fact has a dominant peak at around 2-eV binding energy, which exhibits a strong intensity enhancement in a narrow photon energy region around 70 eV. This is interpreted as a direct transition from the lower band at  $X_6$ , in excellent agreement with the above derivation, an interpretation that is strengthened by observing that in the spectra at slightly lower energies (65 and 60 eV; other spectra in this region are not shown in Fig. 2), the peak at 4-eV binding energy is enhanced in intensity, also pointing to the influence of a large cross section in this region of photon energies, enhanced by the high density of states near the X point. The spectra recorded at higher photon energies are important for the band determination since they give access to the band energies up to the X point. The solid lines in Fig. 3 are from a self-interaction and relaxation-corrected pseudopotential calculation by Vogel, Krüger, and Pollmann,<sup>9</sup> where the Cd 4d electrons are treated as valence electrons; this and other calculational schemes are discussed in terms of their predictive power below. There is generally good agreement between the calculation and our experimental data, although the lowest  $\Sigma_5$  band seems to be somewhat higher in binding energy than predicted by the calculation. The experimental critical point energies are listed in Table I along with the results from various calculational schemes and will be discussed in relation to these below.

Consider now the Cd 4d derived peaks. From the data in Fig. 4(a), we note that here also, considerable changes with photon energy occur in the spectra. A peak towards lower binding energies splits off from the seemingly straightforward spin-orbit split peak, which is seen at  $\hbar\omega = 40$  eV, most clearly seen at  $\hbar\omega = 70$  eV, and the intensity ratio of the central peak pair and its peak shape also undergo considerable change between 40 and 100 eV. The centroid of the peak is located at about 9.5 eV below the VBM, with an average half-width of about 1.5 eV. There has been consid-

TABLE I. Experimentally determined electronic energies (eV) in the valence-band structure and Cd 4d region of zinc blende CdSe, compared with results of calculations (Refs. 9 and 23). Valence bands are counted from the fundamental band gap down.

	Experimental	Christensen (Ref. 23)	Vogel <i>et al.</i> (PP, Ref. 9)	Vogel <i>et al.</i> (SIRC-PP, Ref. 9)
$X_7, X_6$ (band 1 and 2)	-1.85	-1.95, 2.15	-2.0	-2.15, -2.35
$X_6$ (band 3)	-4.0	-4.25	-4.3	-4.7
$\Sigma_{\min}$	-2.25	-2.75	-2.7	-3.0
Cd 4d band, top	-8.6	-10.4	-6.6	-9.3
Cd 4d band, bottom	-9.8	-12.4	-7.9	-10.9

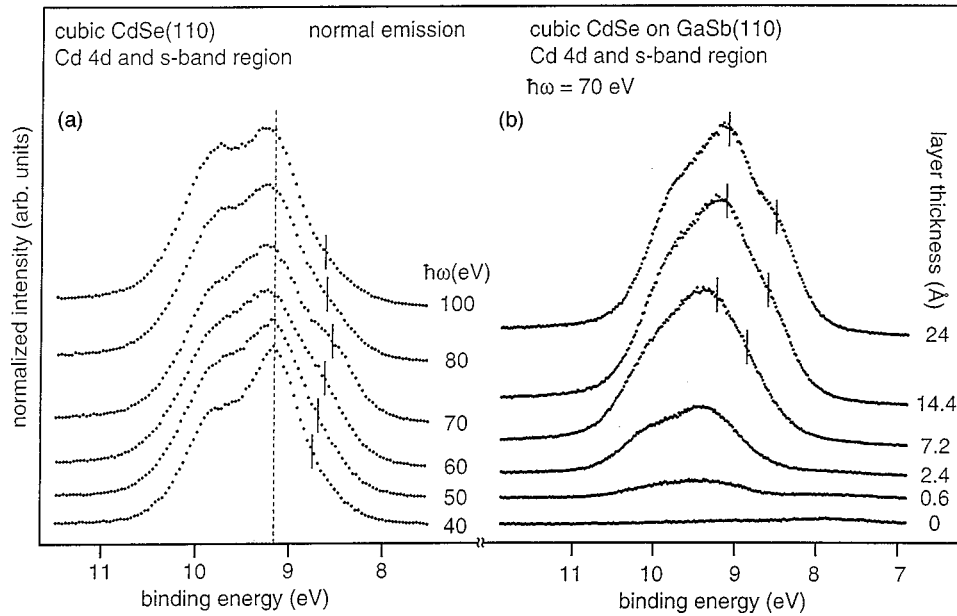


FIG. 4. (a) Variations in peak shape of the Cd 4d peak as a function of photon energy, showing the clear emergence of a shoulder peak around 70-eV photon energy. (b) Evolution of the Cd 4d line shape as a function of layer thickness, demonstrating the emergence of the shoulder peak with thickness (see text).

erable controversy concerning the interpretation of the line shape of the Cd 4d band in the Cd-based II-VI semiconductors, in particular for wurtzite CdSe.<sup>15</sup> Wiklund and co-workers have interpreted the Cd 4d line shape from CdSe(11 $\bar{2}$ 0) in terms of one bulk and one surface-derived core-level emission, similar to the surface core-level shifts that are clearly seen in the cation *d* peaks from Ga and In in the spectrum from the (110) surface of the III-V semiconductors.<sup>16–18</sup> They have interpreted the extra peak or shoulder towards lower binding energies, such as seen in Fig. 4(a), in terms of emission from the selenium 4s band. The shoulder peak in our spectra actually evolves as a function of layer thickness, as seen in Fig. 4(b), and might well be interpreted in terms of a dispersing *s*-like band, the width of which increases as the solid layer builds up towards the full three-dimensional solid. However, an assignment to a Se 4s band appears questionable on the basis of the known relative photoionization cross sections for the Cd 4d and Se 4s bands and also by recourse to band-structure calculations as discussed below. From the tabulated values by Yeh and Lindau<sup>19</sup> it is found that the Se 4s level atomic photoionization cross section is a factor of 200 lower than that of the Cd 4d level. A comparison of the anion *s* levels in the III-V materials<sup>20</sup> suggests that the anion *s*-derived band never has more than a few percent of the intensity of the cation *d* level, e.g., in the comparable case of InP or InSb. Stampfl *et al.*, in their study of cubic CdS,<sup>6</sup> have carried out a linearized muffin-tin orbital calculation and found that the contributions from the sulfur *s* and *p* states in this region amounts to only 5.5% of the total density of states. In the related case of ZnS(110) the sulfur-derived 3s level was also found to be quite weak compared to the Zn 3d states.<sup>21</sup> Another argument against the interpretation of the Cd 4d line shape in terms of a bulk and surface core level and an overlapping anion *s* band is drawn from the band-structure calculations, all of which predict a considerable dispersion in the *d* levels.

Finally, the SIRC-PP calculations by Vogel, Krüger, and Pollmann, which agree quite well with the experimental results as far as the energy of the 4d level is concerned, place the Se 4s band more than 3 eV below the center of gravity of the Cd 4d bands. Thus we interpret the emergence of an extra peak at about 70 eV as the lowest binding energy *d* band, which in fact is seen to have a rather large dispersion, about 0.9 eV; this band actually has an *s*-like dispersion, i.e., the highest binding energy is at the  $\Gamma$  point. Thus the fact that the shoulder grows out of the main group of Cd 4d peaks as a function of coverage suggests that, as the CdSe layer builds up towards the full three-dimensional solid, the dispersion width of the uppermost *d* band increases.

Since there is a total of five *d* bands away from the high symmetry points, and these are closely spaced and rather broad, it is unlikely that one will be able to separate all of these in the type of experimental band-structure determination such as successfully carried out above for the *s-p* valence bands. However, one can attempt to compare the overall line shape with a density of states derived from the band-structure calculation. Such data were made available to us by Vogel, Krüger, and Pollmann, and a comparison of the experimental spectrum at  $\hbar\omega = 70$  eV with a Lorentzian-broadened density of states in the Cd 4d region is shown in Fig. 5. It is apparent that the dominant peak and the shoulder towards high binding energy coincide with the two main peaks of the density of states, while the third *d*-derived peak, dispersing towards lower binding energy, is located where the shoulder in the spectrum appears towards lower binding energy. We have not attempted a fit to the experimental line shape on the basis of a free Gaussian or Lorentzian broadening parameter, since no extra information on the quality of the band dispersion in the calculation can be gained. From the band-structure calculation of Vogel, Krüger, and Pollmann, depicted in Fig. 4, we note that while the two main groups of the *d* bands have only a small dispersion, one band

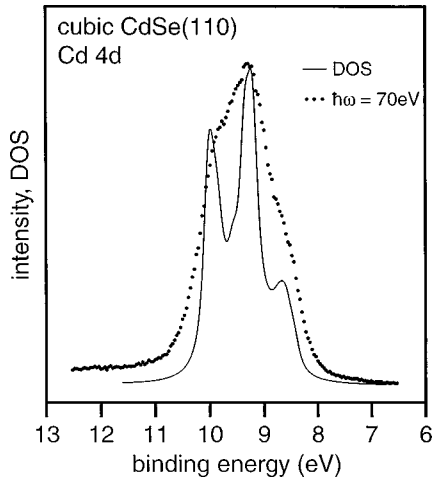


FIG. 5. Comparison of the Cd  $4d$  line shape at a photon energy of 70 eV, with the broadened density of states calculated in the SIRC-PP scheme by Vogel *et al.*, showing that the peaks and shoulders in the experimental spectrum match the structures in the calculated DOS.

in each of the groups has a much larger dispersion, which causes this peak in the density of states. The dispersion of the equivalent band in the lower group of bands causes the gap between the two groups of bands to fill up around the  $K$  point. This influence is responsible for the changes in the main peak shape between 40- and 110-eV photon energy. The experimental observations can therefore be consistently described in terms of a bandlike behavior of the  $d$  states alone. Whether the anion  $s$  state coincides in energy with the  $d$  states, or is situated at higher binding energy, cannot be resolved on the basis of these data.

As mentioned above, the width of the Cd  $4d$  peak, and the variations in peak shape upon variation of the photon energy has been regarded as evidence for a surface core-level shift, and one can in fact achieve a reasonable line-shape analysis based on two spin-orbit doublets, but an extra single peak (the ‘‘anion  $s$  peak’’) is then needed in order to take care of the low-energy shoulder. Here we take a different point of view, by interpreting the peak shape changes as due to bandlike behavior. Initial state shifts, caused by a different Madelung potential at the surface, and/or through the rotation-relaxation of the surface, require a level in which the transferred charge is localized. Delocalized states, in which charge is spread out over several unit cells, or band states, will not suffer such discrete shifts. Consider the  $4d$  levels of the neighboring elements Ag, Cd, and In. The Ag  $4d$  states in AgBr (binding energy about 3.5 eV) have a maximum dispersion of about 1 to 1.4 eV and may thus be classified as band states. The In  $4d$  states in InP, for example, with a binding energy of 17 eV, do not exhibit dispersion, and exhibit a clear surface core-level shift.<sup>17</sup> The Cd  $4d$  states are in between these two extremes, and constitute a case of weak dispersion. The best model to apply, core level or band, obviously depends on the character of the wave functions of the states involved, and in the absence of detailed calculations one can only speculate as to what extent the Cd  $d$  levels will be influenced by the charge redistribution at the surface.

While the predictions of the band-structure calculations for the upper valence band are usually supported by experi-

ment as discussed below, binding energies of the deeper bands—shallow core levels are often in error by several electron volts. Progress has recently been made, however, in dealing with some of the shortcomings of density functional calculations (DFT) using the local density approximation (LDA) for correlation and exchange. Such calculations, which are largely based on ‘‘state-of-the-art’’ nonlocal pseudopotentials, have led to remarkable results in band-structure calculations. However, they suffer from the fact that the fundamental band gap is usually underestimated by 50% or more; in the case of ZnO, the calculated band gap within LDA is 0.23 eV, while the experimental value is 3.4 eV.<sup>9</sup> LDA also fails to correctly describe strongly localized semi-core-like  $d$  states and their binding energies. For the II-VI semiconductors, the binding energy of the  $d$  states is usually about 3 eV too low as compared with experiment. This is partly due to an unphysical self-interaction and to the neglect of electronic relaxation that is contained in any standard LDA calculation. This causes their interaction with the anion  $p$  states to be artificially enhanced, affecting the dispersion of these states and pushing them closer to the conduction bands. While it is possible to deal with such problems by including the  $d$  electrons in a calculation based on the  $GW$  approximation, this is only computationally feasible in simple cases. Several groups have taken the alternative path of including *atomic* self-interaction corrections and electronic relaxation into the pseudopotentials that are used in LDA calculations. Once these pseudopotentials are constructed, the calculations can proceed within the usual LDA framework, greatly simplifying the evaluation. For the present case of cubic CdSe, Vogel, Krüger, and Pollmann have compared the results for standard and SIRC-PP pseudopotentials. They find an average  $d$ -band energy of  $-7.4$  eV for the standard case, and  $-10.4$  eV for the SIRC-PPs, in good agreement with our experimental value of  $-9.7$  eV (see also Table I). This lowering of the  $d$  band also has a pronounced influence on the dispersion of the lowest  $p$ -derived valence band: in a comparative calculation for ZnO, the lowest  $p$  band was found to disperse to about 1.3 eV higher binding energies when calculated with the uncorrected pseudopotentials. One might speculate that a slight overestimation of self-interaction and relaxation could have shifted the  $d$  bands too high in binding energy, such that the lowest  $p$  band also gains a dispersion that is larger than found in experiment.

As expected, the improvement in agreement is not as large when we consider the upper,  $p$ -like bands. Here, the empirical tight-binding calculation of Wang and Duke<sup>22</sup> gives good agreement already, not surprisingly perhaps, being based on optical absorption data (no data are given for the Cd  $4d$  bands). The linearized muffin-tin orbital calculation by Christensen<sup>23</sup> also represents the  $p$  bands well, with even better agreement than the SIRC-PP calculations of Vogel, Krüger, and Pollmann for the bands at the  $X$  point (see Table I) and at  $\Sigma_{\min}$ , the maximum binding energy of the second band.

In summary, we have studied the band structure of cubic CdSe along the  $\Gamma$ - $K$ - $X$  direction. Good agreement with recent band-structure calculations is found, even for the problematic Cd  $4d$  states. Instead of assigning a structure in the Cd  $4d$  band to Se  $4s$  emission as previously suggested, we

relate it to a strongly dispersing part of the Cd 4*d* bands, in agreement with a density-of-states calculation.

#### ACKNOWLEDGMENTS

This work was supported by the Bundesministerium für Bildung, Forschung, und Technologie under Grant No. 05

622 OLA, and by the Swedish Natural Science Research Council. K.O.M. and D.A.E. appreciate the hospitality of the Fritz-Haber-Institute during their stay, and the help of H. Haak with the technical preparation. We thank J. Pollmann and D. Vogel for stimulating discussions, and for making their data available to us prior to publication.

\*Present address: Dresdner Bank AG, KS FC IR, 60301 Frankfurt, Germany.

<sup>1</sup>M. Jain, in *II–VI Semiconductor Compounds* (World Scientific, Singapore, 1993).

<sup>2</sup>P. Hofmann, K. Horn, A. M. Bradshaw, D. Fuchs, M. Cardona, and R. L. Johnson, *Phys. Rev. B* **47**, 1639 (1993).

<sup>3</sup>W. G. Wilke and K. Horn, *J. Vac. Sci. Technol. B* **6**, 1211 (1988).

<sup>4</sup>W. G. Wilke, R. Seedorf, and K. Horn, *J. Vac. Sci. Technol. B* **7**, 807 (1989).

<sup>5</sup>N. G. Stoffel, *Phys. Rev. B* **28**, 3306 (1983).

<sup>6</sup>A. P. J. Stampfl, P. Hofmann, O. Schaff, and A. M. Bradshaw, *Phys. Rev. B* **55**, 9679 (1997).

<sup>7</sup>G. Neuhold, K. Horn, K. O. Magnusson, and D. A. Evans, *J. Vac. Sci. Technol. A* **13**, 666 (1995).

<sup>8</sup>M. Rohlfling, P. Krüger, and J. Pollmann, *Phys. Rev. Lett.* **75**, 3489 (1995).

<sup>9</sup>D. Vogel, P. Krüger, and J. Pollmann, *Phys. Rev. B* **54**, 5495 (1996); (private communication).

<sup>10</sup>T. C. Chiang and D. E. Eastman, *Phys. Rev. B* **22**, 2940 (1980).

<sup>11</sup>L. Sorba, V. Hinkel, H. U. Middelmann, and K. Horn, *Phys. Rev. B* **36**, 8075 (1987).

<sup>12</sup>G. P. Williams, F. Cerrina, G. J. Lapeyre, J. Anderson, R. J. Smith, and J. Hermanson, *Phys. Rev. B* **34**, 5548 (1986).

<sup>13</sup>F. J. Himpfel, *Appl. Opt.* **19**, 3964 (1980).

<sup>14</sup>K. O. Magnusson and S. A. Flodstrom, *Phys. Rev. B* **38**, 5384 (1988).

<sup>15</sup>S. Wiklund, Ph.D. thesis, Lund University, 1993.

<sup>16</sup>D. E. Eastman, T.-C. Chiang, P. Heimann, and F. J. Himpfel, *Phys. Rev. Lett.* **45**, 656 (1980).

<sup>17</sup>W. G. Wilke, V. Hinkel, W. Theis, and K. Horn, *Phys. Rev. B* **40**, 9824 (1989).

<sup>18</sup>A. B. McLean and R. Ludeke, *Phys. Rev. B* **39**, 6223 (1989).

<sup>19</sup>J. J. Yeh and I. Lindau, *At. Data Nucl. Data Tables* **32**, 1 (1985).

<sup>20</sup>L. Ley, R. A. Pollak, F. R. McFeely, S. P. Kowlaczyk, and D. A. Shirley, *Phys. Rev. B* **9**, 600 (1974).

<sup>21</sup>S. R. Barman, S.-A. Ding, K. H. Horn, D. Wolfram, P. Bailey, and D. A. Evans (unpublished).

<sup>22</sup>Y. R. Wang and C. B. Duke, *Phys. Rev. B* **37**, 6417 (1988).

<sup>23</sup>N. E. Christensen (private communication).